ACADEMIC PRESS

Available online at www.sciencedirect.com

SCIENCE DIRECT®

Journal of Sound and Vibration 265 (2003) 745–763

JOURNAL OF SOUND AND VIBRATION

www.elsevier.com/locate/jsvi

Approximate computation of non-linear effects in a vibrating cracked beam

E. Luzzato*

Département Analyses Mécaniques et Acoustiques, EDF R&D, 1, Avenue du Général de Gaulle, 92141 Clamart Cedex, France

Received 5 March 2001; accepted 7 August 2002

Abstract

Crack detection made by the observation of structural dynamic responses has been implemented for several years in non-destructive control using ultrasound transducers. More recently, detection methods have been proposed based upon the analysis of modal properties. As it has been shown that the modal frequencies are not very sensitive to the presence of a breathing crack, alternative detection techniques have been proposed. They are based upon the analysis of the dynamic non-linear effects of the crack. These effects essentially fall into two categories: the harmonic lobes of the main pure tone or modal excitations and the modulation lobes between these excitations. In order to test them, various simulation methods can be used. This paper presents the test of two simple one-dimensional finite element models and the comparison of their results with a two-dimensional finite element model for the representation of the stiffness loss of an open crack as well as the non-linear behaviour of a breathing crack. The configuration considered is a simply supported beam with a crack at its middle point. Two distinct damage rates are proposed as descriptors to characterize the presence of the crack in the beam: the harmonic damage rate and the modulation damage rate. It is found that the simple one-dimensional models can accurately determine the damage rates associated with the breathing crack, when compared to the results obtained with the two-dimensional model. It is also found that the proposed damage rates can be efficiently used as descriptors of the presence of a crack as their magnitude increases faster than the crack size and in a monotonic way.

*Tel.: +33147653706; fax: +33147653692.
E-mail address: emile.luzzato@edf.fr (E. Luzzato).

0022-460X/03/$ - see front matter
doi:10.1016/S0022-460X(02)01562-6

1. Introduction

The non-linear effects of vibrating cracked beams are well known and many authors proposed various measurement methods for crack detection, which essentially fall into three categories: modal perturbation, harmonic lobes and modulation lobes.

The analysis and numerical modelling of eigenfrequency shifts due to the presence of an open crack has been dealt with in the case of a Euler–Bernoulli beam [1,2] and other configurations involving laminated composite materials [3]. Methods to identify the crack size and location from the modal perturbation have also been proposed [4–6]. The effects of crack size on the first eigenfrequency of a prestressed beam have been examined [7], and the authors showed that there is significant coupling between the axial prestress load and the crack size. As industrial structures are generally prestressed, the accurate prediction of the modal perturbation due to the crack without knowing the exact prestressing conditions is difficult. Recently, the vibration response of a beam with a breathing crack was examined by using a given continuous non-linear representation of the mechanical behaviour generated by the crack [8]. The first eigenfrequency was evaluated for various crack sizes assuming this specific non-linear continuous behaviour. For this computation, the change in flexibility of the open-crack beam has been derived from a polynomial expansion proposed in Ref. [9].

The analysis of harmonic lobes generated by acoustic energy emission in damaged bars was first investigated in Refs. [10,11]. Concerning damaged rotating shafts, various crack models have been developed from traditional fracture mechanics theory [12,13]. These studies showed that the presence of a crack could be identified by the observation of the second harmonic of the rotating frequency. Its non-linear effects generally lead to a strong increase of the second harmonic magnitude whereas the first harmonic is more affected by an unbalance phenomena. Later, a method was proposed [14] for the detection of cracks in rotating shafts based on long term monitoring of the second and third harmonics response magnitudes as it was shown that they all increase in direct proportion to crack size.

Recently, the use of vibro-acoustic modulation lobes to detect cracks in structures has been emphasized [15–20]. The methods examine the non-linear effects generated by the breathing crack. These observed effects are essentially the non-linear interaction between the ultrasonic probing signal and the low-frequency vibrations of the cracked beam. Various materials have been tested and the results showed that the method can be quite reliable for a non-destructive testing process.

This paper presents an analysis of the approximation made by using two simple one-dimensional models to simulate the stiffness loss of an open crack as well as the non-linear behaviour of a breathing crack in a beam. A two-dimensional finite element model has also been developed as a reference model. The two basic one-dimensional finite element models are examined and their stiffness loss due to the open crack is tuned by fitting their first eigenfrequencies with those of at the two-dimensional model. The fitting process uses simple approximations for the relationship between the first eigenfrequencies and the open-crack rate. The dynamic behaviour of the breathing crack is then modelled within the frame of a bilinear constitutive law. With the three proposed models, the relationship between eigenfrequencies and crack rate for a breathing crack is investigated and the results are compared. The computation of the non-linear effects resulting from a breathing crack leads to the proposal of two descriptors

that may allow one to detect the early presence of a breathing crack: the harmonic damage rate and the modulation damage rate.

2. Approximation of the relationship between the eigenfrequencies and the open-crack rate

The geometrical crack rate is represented by α_o

$$\alpha_o = \frac{h_c}{h}, \tag{1}$$

where h_c is the geometrical depth of the crack, and h is the thickness of the undamaged beam (see Fig. 1).

In this section, it is intended to propose parametered functionals to accurately approximate the variation of the first eigenfrequencies of beams in bending vibrations with a radial open crack. The approximation functional can then be used to derive the so-called 1-D equivalent crack rate as a function of the geometrical crack rate. The 1-D equivalent crack rate represents the loss of rigidity that one should impose onto the 1-D model in order to match the variation of the first eigenfrequencies of the 2-D model, considered here as a reference model.

Three finite element numerical models are being considered: one two-dimensional model denoted 2-D and two one-dimensional models, respectively, denoted '1-D-EF' and '1-D-SPR'.

In the 2-D model, the bending beam is discretized by means of plate elements with in-plane deformations. The discretization mesh of the 2-D model is chosen to be regular and consists of 1060 rectangular plate elements. A mesh refinement is generated at the location of the crack for a satisfactory representation of the strain energy distribution. The crack geometry is simulated by extracting refined elements at the crack location. The depth of the crack is therefore obtained by extracting 0 to 7 elements such that α_o varies from 0 to 0.7 with a step of 0.1. The crack is located at the middle point of the beam as shown in Fig. 1.

In both 1-D models, the beam is discretized with identical beam finite elements. Except at the crack location, the discretization mesh of both 1-D-EF and 1-D-SPR models constituted of 50 regular beam elements.

In the 1-D-EF model, the stiffness loss is represented by means of one single modified beam finite element. The cross-sectional moment of inertia of that beam element is chosen as the parameter that allows one to match the modal behaviour of the 2-D model with a open crack. The corresponding matching procedure is presented in Section 2.2.

In the 1-D-SPR model, the stiffness loss is represented by means of a bending spring connecting both sides of the beam. The spring stiffness is chosen as the parameter that allows one to match the modal behaviour of the 2-D model with a open crack. The corresponding matching procedure is presented in Section 2.3.

For the numerical applications, the beam considered is chosen simply supported at its ends, such that its length $L = 1$ m, its width $b = 0.02$ m, its thickness $h = 0.05$ m, its density $\rho = 7850\ \mathrm{kg\ m^{-3}}$, its Young's modulus $E = 2.0 \times 10^{11}\ \mathrm{N\ m^{-2}}$ and the Poisson ratio $\nu = 0.29$.

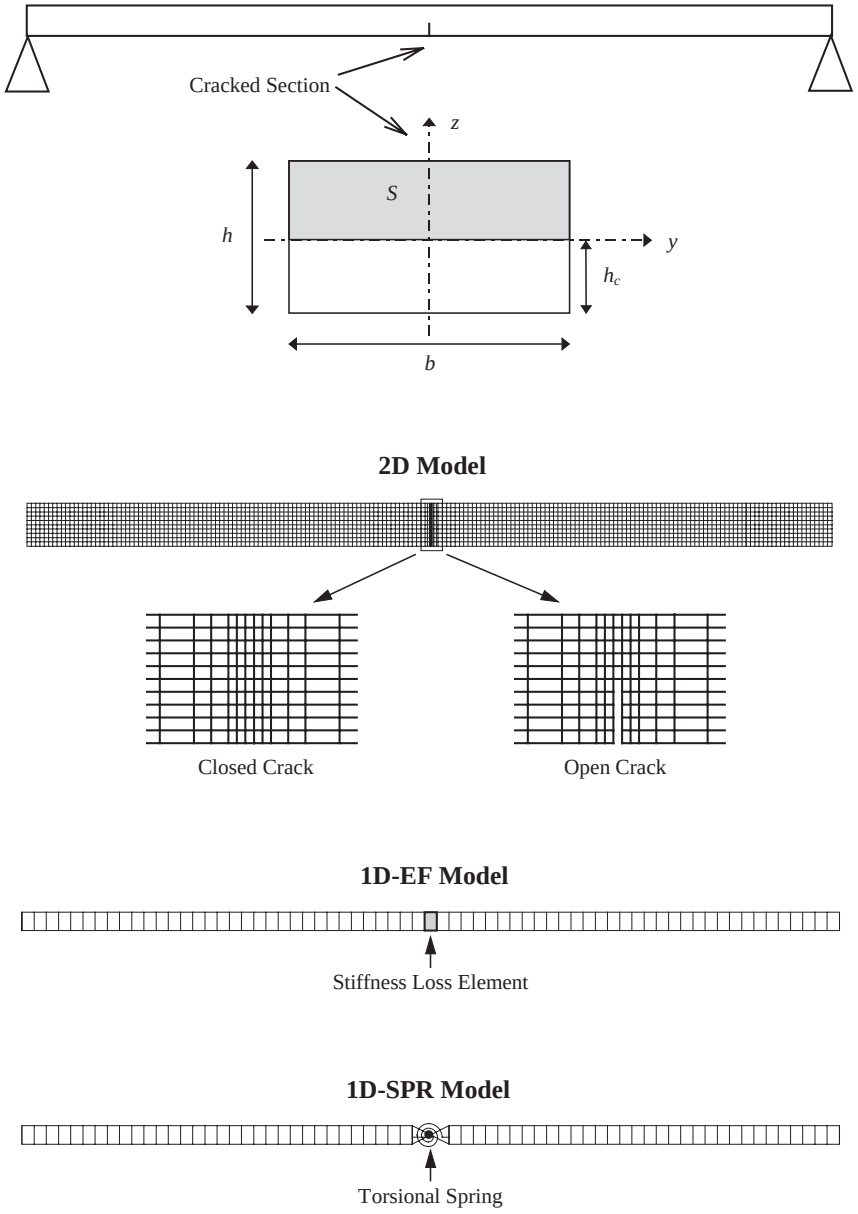

Fig. 1. Cracked beam configuration and the three numerical models considered.

2.1. Eigenfrequency approximation for the 2-D model

The eigenfrequencies computed with the 2-D model of the beam are determined for eight successive values of geometrical crack rate α_o. It has been shown [21] that the evolution of the beam eigenfrequency f_i of rank i determined in term of its stiffness, and in this case, in term of α_o,

Table 1
2-D model—parameters of approximation (2) proposed for the reduced eigenfrequencies of the open-crack beam

Mode i	Parameter q_{1i}	Parameter q_{2i}	Maximum error on $\tilde{f}_i$ (%)
1	2.3518	1.3908	0.218
2	3.3939	230.86	5.54×10^{-4}
3	1.8813	2.5753	0.253
4	3.4036	63.426	1.80×10^{-3}
5	1.7588	3.3680	0.213
6	3.4380	31.468	3.13×10^{-3}
7	2.3228	2.1866	0.295
8	3.5008	19.498	8.19×10^{-3}

can generally be accurately approximated by the following parametered relationship:

$$\tilde{f}_i(\alpha_o, q_{1i}, q_{2i}) \approx 1 - \frac{\alpha_o^{q_{1i}}}{\alpha_o^{q_{1i}} + q_{2i}}, \tag{2}$$

where

$$\tilde{f}(\alpha_o) = \frac{f_i(\alpha_o)}{f_i(\alpha_o = 0)}, \tag{3}$$

is the reduced eigenfrequency of the 2-D model; by definition, they always have positive values less than 1.

Parameters q_{1i} and q_{2i} are determined by minimizing the following quadratic form:

$$\varepsilon_i(q_{1i}, q_{2i}) = \sum_{j=1}^{n} \left(1 - \frac{\tilde{f}(\alpha_{0j}, q_{1i}, q_{2i})}{f_i^0(\alpha_{0j})} \right)^2, \tag{4}$$

where $f_i^0(\alpha_{0j})$ is the reduced eigenfrequency computed with the 2-D finite element model for geometrical crack rate α_{0j}.

Table 1 presents parameters q_{1i} and q_{2i} for the first eight flexural eigenfrequencies of the beam.

The proposed approximation which may be considered as satisfactory as the maximum error for the first eight reduced eigenfrequencies, is less than 0.3%. Fig. 2 presents the evolution of these eigenfrequencies as functions of the open-crack rate, obtained by means of the 2-D finite element model on one hand, and approximation (2), on the other hand. These results illustrate the good accuracy obtained with the proposed approximation (2).

2.2. Approximation for the 1-D-EF model

With the 1-D-EF model, the cross-sectional moment of inertia at the crack point is the parameter used to match the first modal frequencies of the 2-D model. It may be written as

$$I = I_o(1 - \alpha^\beta), \tag{5}$$

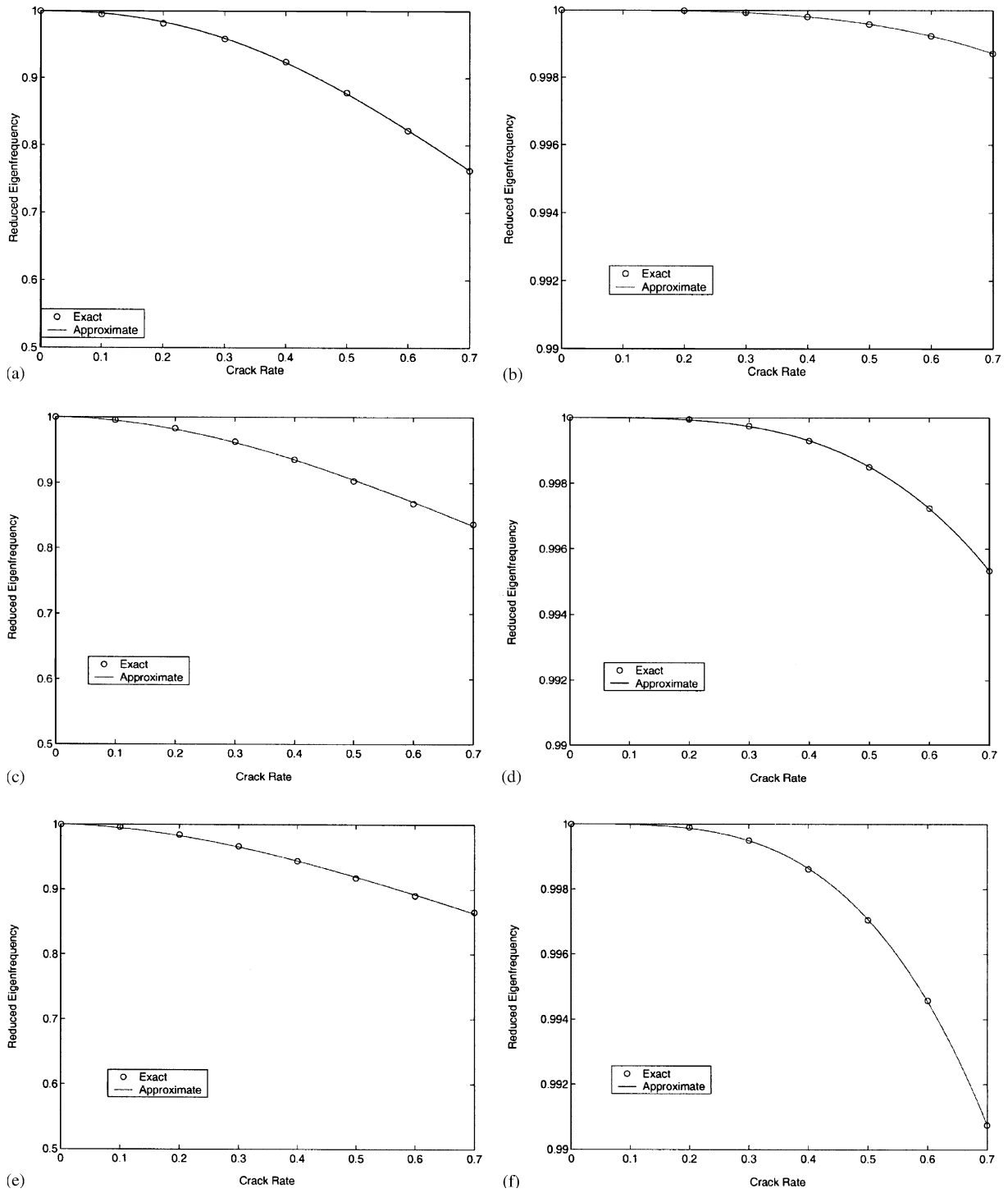

Fig. 2. 2-D model—exact and approximated computation of reduced eigenfrequencies evolution as functions of the open-crack rate: (a) mode 1, (b) mode 2, (c) mode 3, (d) mode 4, (e) mode 5, (f) mode 6, (g) mode 7, (h) mode 8.

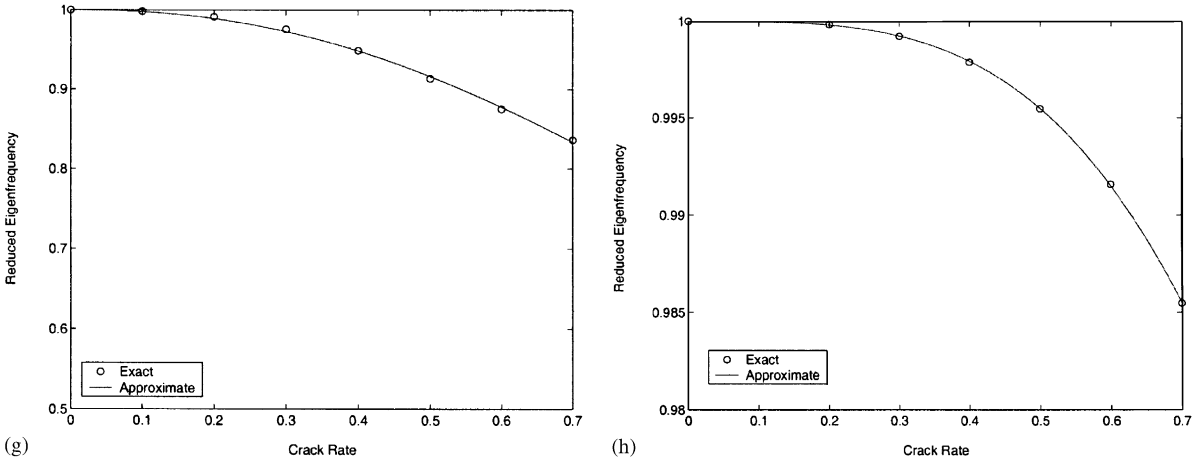

Fig. 2 (*continued*).

Table 2
1-D-EF model—parameters of approximation (6) proposed for the odd reduced eigenfrequencies of the open-crack beam

Mode i	Parameter p_{1i}	Parameter p_{2i}	Parameter p_{3i}	Maximum error on $\tilde{f}_i$ (%)
1	1.3244×10^{-3}	-1.8033×10^{-4}	-1.5184×10^{-4}	0.253
3	1.3454×10^{-3}	-4.5862×10^{-4}	-1.5460×10^{-4}	0.225
5	5.7961×10^{-3}	-3.2693×10^{-3}	-6.7454×10^{-4}	0.192
7	1.6677×10^{-3}	-1.3125×10^{-3}	-1.9369×10^{-4}	0.174

where β is a coefficient arbitrarily chosen equal to 0.1 so that the range of magnitude of the 1-D-EF reduced eigenfrequency is of the same order as the range of magnitude of the 2-D reduced eigenfrequency. The various computation that were performed showed that the reduced eigenfrequency evolution of the 1-D-EF model, determined in terms of α, can be accurately approximated by the following parametered relation:

$$\tilde{f}_i(\alpha, p_{1i}, p_{2i}, p_{3i}) \approx 1 - p_{3i} \frac{\alpha^{p_{1i}}}{\alpha^{p_{1i}} - 1 + p_{2i}}. \tag{6}$$

Parameters p_{1i}, p_{2i} and p_{3i} are determined by minimizing the quadratic form (4) in which $f_i^0(\alpha_j)$ represents the eigenfrequency computed with the 1-D-EF model. Table 2 presents the values found for parameters p_{1i}, p_{2i} and p_{3i} of relation (6), for the first odd eigenfrequencies of the 1-D-EF model. As the crack is located at the middle point of the beam, the 1-D-EF model does not lead to any change of its even eigenfrequencies.

The maximum error is less than 0.3% for the first odd eigenfrequencies being considered.

Fig. 3 presents the evolution of the first odd reduced eigenfrequencies of the bending beam as a function of the open-crack rate, obtained by means of the 1-D-EF finite element model on one

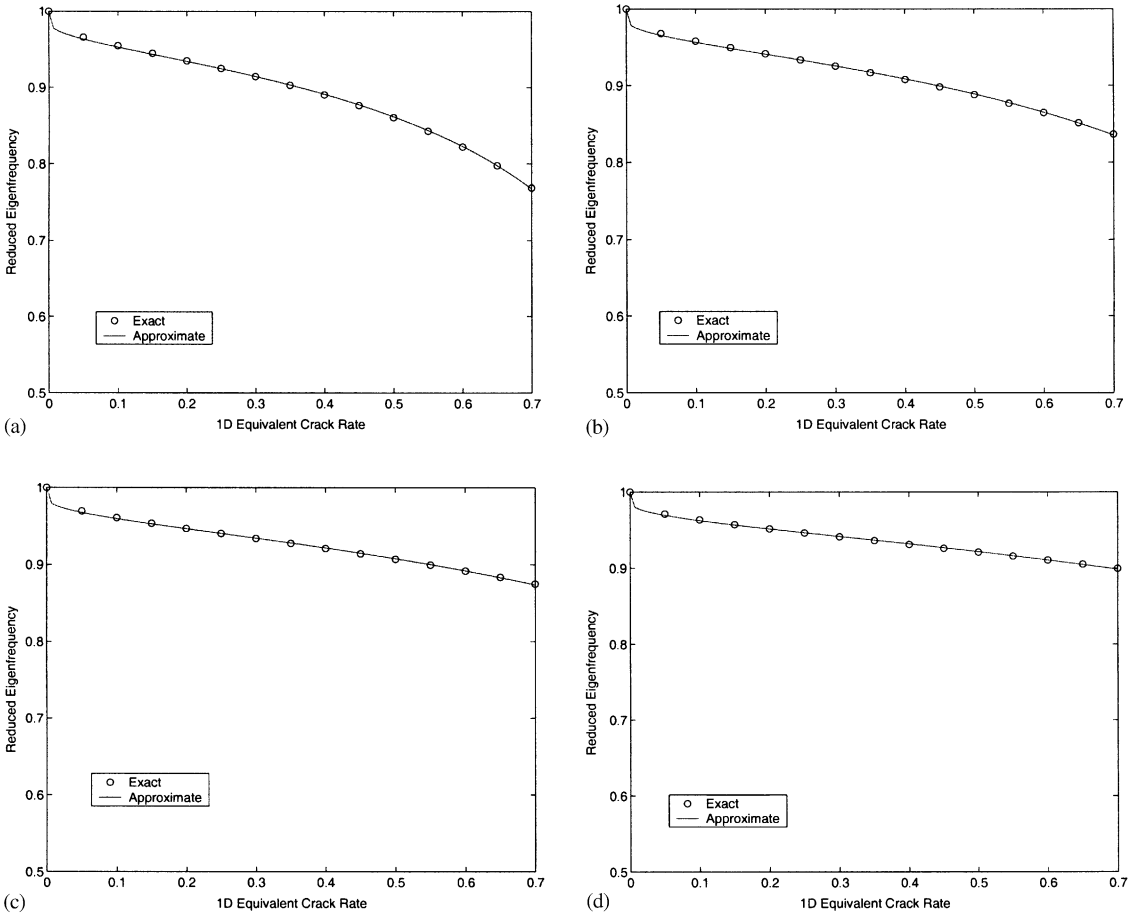

Fig. 3. 1-D-EF model—exact and approximated computation of reduced eigenfrequencies evolution as functions of the open-crack rate: (a) mode 1, (b) mode 3, (c) mode 5, (d) mode 7.

hand, and with approximation (6) on the other hand. The approximations realized are quite satisfactory.

As relation (6) is simple enough, it can easily be inverted so that one gets

$$\alpha_i^{\beta} = \left((p_{2i} - 1) \frac{\tilde{f}_i - 1}{1 - \tilde{f}_i - p_{3i}} \right)^{\beta/p_{1i}}, \tag{7}$$

where α_i^{β} denotes the 1-D-EF equivalent crack rate associated to eigenfrequency of rank i obtained with the 1-D-EF model. Requiring the reduced eigenfrequency of the 1-D-EF model to be equal the corresponding eigenfrequency of the 2-D model in Eq. (2), expression (7) leads to the equivalent crack rate of model 1-D-EF as follows:

$$\alpha_i^{\beta} = \left((p_{2i} - 1) \frac{\alpha_o^{q_{1i}}}{q_{2i} p_{3i} - \alpha_o^{q_{1i}} (1 - p_{3i})} \right)^{\beta/p_{1i}}, \tag{8}$$

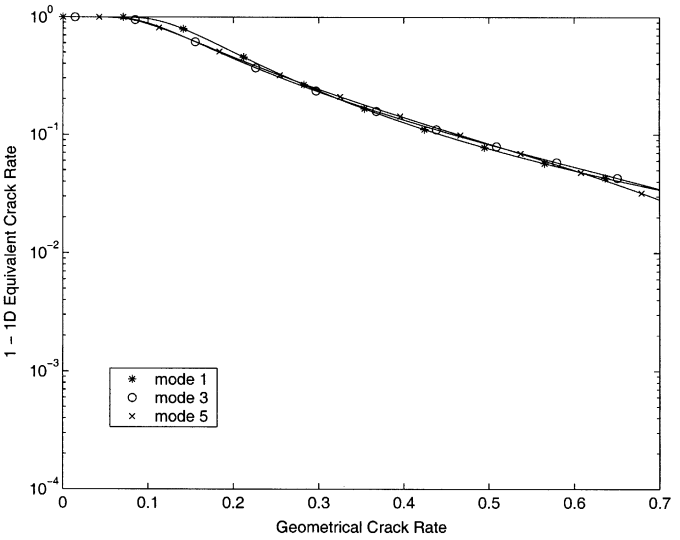

Fig. 4. 1-D-EF model—equivalent crack rate expressed as a function of the geometrical open-crack rate for the first odd eigenfrequencies.

so that the bending cross-section inertia of the element representing the crack may be written as

$$I_i = I_o(1-\alpha_i^{\beta}) = I_o\left(1-\left((p_{2i}-1)\frac{\alpha_o^{q_{1i}}}{q_{2i}p_{3i}-\alpha_o^{q_{1i}}(1-p_{3i})}\right)^{\beta/p_{1i}}\right). \tag{9}$$

If this bending cross-section inertia is imposed on the 1-D-EF element that represents the crack, then the variation with respect to α_i of the ith reduced eigenfrequency of the 1-D-EF model accurately matches the variation with respect to α_o of the ith reduced eigenfrequency of the 2-D model. Fig. 4 illustrates relation (8) for the first odd eigenfrequencies of the cracked beam in bending vibrations with the 1-D-EF model.

The curves obtained for the equivalent crack rate of the 1-D-EF model, as a function of the geometrical crack rate, are monotonic increasing curves. However, they are slightly different for each odd number mode. The attempt to represent the stiffness loss of a beam cracked on one side by means of a one-dimensional model, symmetric by definition, may explain these differences. Nevertheless, this result illustrates the ability of this 1-D-EF model to accurately represent the behaviour of a beam with a open crack in bending vibrations. The equivalent crack rates obtained for the first three odd eigenfrequencies are very close, in the 0.1–0.7 range of variation of the geometrical crack rate.

2.3. Approximation for the 1-D-SPR model

With the 1-D-SPR model, the spring stiffness at the crack point is the parameter used to match the first modal frequencies of the 2-D model. It may be written as

$$K_{Mi} = K_{Mo}(1-\alpha^{\beta}). \tag{10}$$

Table 3
1-D-SPR model—parameters of approximation (6) proposed for the odd reduced eigenfrequencies of the open-crack beam

Mode i	Parameter p_{1i}	Parameter p_{2i}	Parameter p_{3i}	Maximum error on $\tilde{f}_i$ (%)
1	3.2448×10^{-3}	-4.7694×10^{-4}	-3.3698×10^{-4}	1.19×10^{-2}
3	3.0116×10^{-3}	-1.0166×10^{-3}	-3.1571×10^{-4}	8.84×10^{-3}
5	1.9036×10^{-2}	-1.0678×10^{-2}	-2.0729×10^{-3}	8.05×10^{-3}
7	2.7732×10^{-2}	-2.2245×10^{-2}	-3.1219×10^{-3}	8.95×10^{-3}

The same approximation process as the one used for the 1-D-EF model has been implemented for the 1-D-SPR model. Table 3 presents the values found for parameters p_{1i}, p_{2i} and p_{3i} in relation (6), for the first odd eigenfrequencies obtained with the 1-D-SPR model.

For the first four eigenfrequencies of odd number rank, the approximation leads to a maximum error of less than 0.012%. Fig. 5 presents the evolution of these first odd reduced eigenfrequencies as functions of the crack rate, obtained by means of the 1-D-SPR finite element model on one hand, and with approximation (6), on the other hand.

The approximations obtained are quite satisfactory. Expression (6) derived in the previous section, applied also for the 1-D-SPR model. In this case, the spring flexural stiffness K_M is expressed as a function of the equivalent crack rate α_i:

$$\begin{aligned} K_{Mi} &= K_{Mo}(1-\alpha_i^{\beta}) \\ &= K_{Mo}\left(1-\left((p_{2i}-1)\frac{\alpha_o^{q_{1i}}}{q_{2i}p_{3i}-\alpha_o^{q_{1i}}(1-p_{3i})}\right)^{\beta/p_{1i}}\right). \end{aligned} \tag{11}$$

For the 1-D-SPR model, β is a coefficient arbitrarily chosen to be equal to 2.0×10^{-3} so that the range of magnitude of the 1-D-SPR reduced eigenfrequency is of the same order as the range of magnitude of the 2-D reduced eigenfrequency.

Fig. 6 illustrates relation (11) for the first odd eigenfrequencies of the beam with an open crack represented by the 1-D-SPR model.

The curves obtained for the equivalent crack rate of the 1-D-SPR model, as a function of the geometrical crack rate are monotonic increasing curves. As for the 1-D-EF model, they are slightly different for each odd number mode. These differences are larger than those of the 1-D-EF model for small values of the geometrical crack rates being typically between 0 and 0.2. As the crack is represented by a simple bending moment spring, it does not account for the stiffness loss in shearing force at the crack point; this may explain the curve differences for the early crack rates. For crack rates beyond 0.2, this result illustrates the ability of this 1-D-SPR model to accurately represent the behaviour of a beam with a open crack in bending vibrations.

3. Analysis of the relationship between eigenfrequencies and crack rate for a breathing crack

The results obtained in the previous section allow one to compute, by means of each considered model, impulse responses of the bending cracked beam. For the 2-D model, the breathing crack

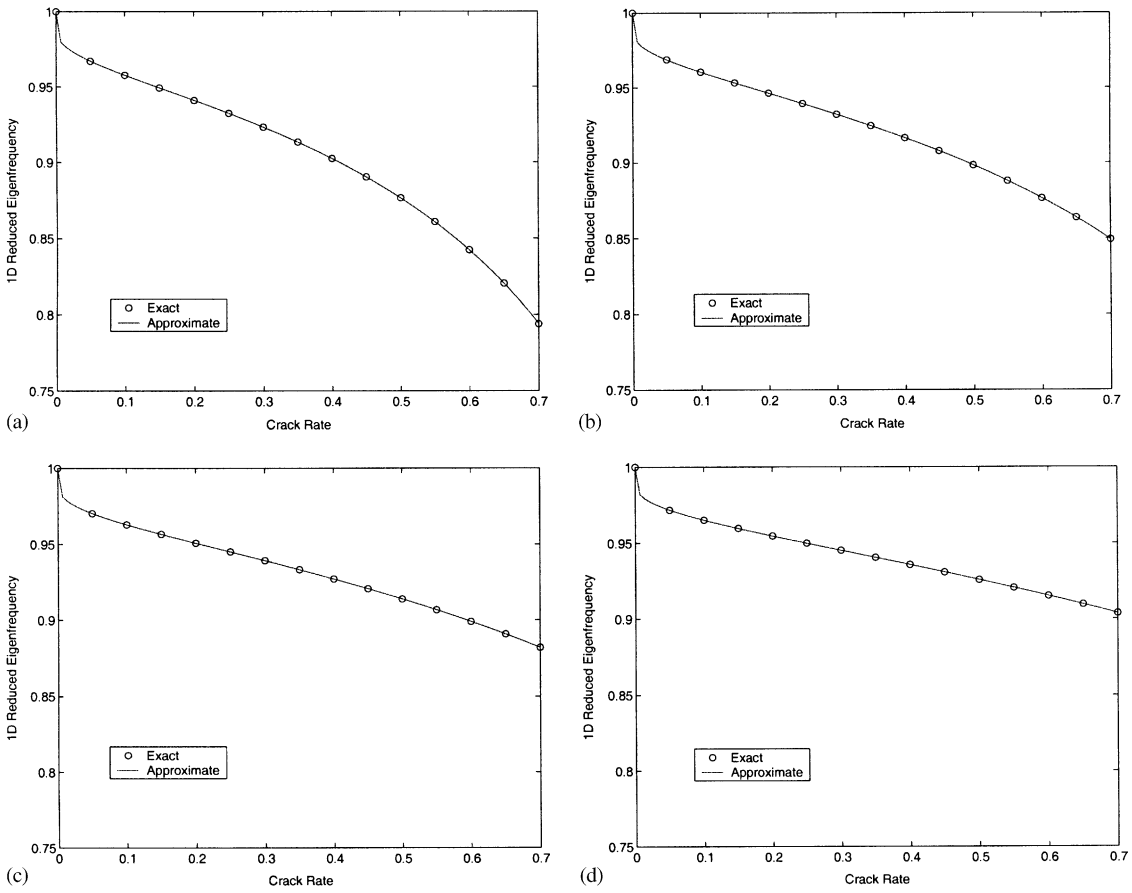

Fig. 5. 1-D-SPR model—exact and approximated computation of reduced eigenfrequencies evolution as functions of the open-crack rate: (a) mode 1, (b) mode 3, (c) mode 5, (d) mode 7.

behaviour is simulated by means of a bilinear model. Depending upon the relative positions of both crack edges, either a closed- or a open-crack configuration can be considered. The non-linear time computation is made by projecting the displacement degrees of freedom on to the two modal bases of the 2-D model, alternately the open-crack and the closed-crack modal bases, according to the relative displacements of both crack edges at the surface of the beam. The results of this type of representation has been compared with the results obtained with a more sophisticated model where the breathing crack behaviour is modelled by contact springs distributed on the length of the 2-D crack. For the first modes, the computed behaviour remains in very good agreement. However, the computation time of the bilinear model is much smaller by a factor 10.

For both 1-D models, either an open- or closed-crack configuration is selected depending upon the value of the second order derivative of the deflection at the crack point. This derivative is estimated as a function of the displacements and slopes of the closest mesh nodes. The non-linear time computation is also made by projecting the displacement degrees of freedom on to the two modal bases of the 1-D model considered, alternately the open-crack and the closed-crack modal bases, according to the second order derivative of the deflection at the crack point. The analysis of

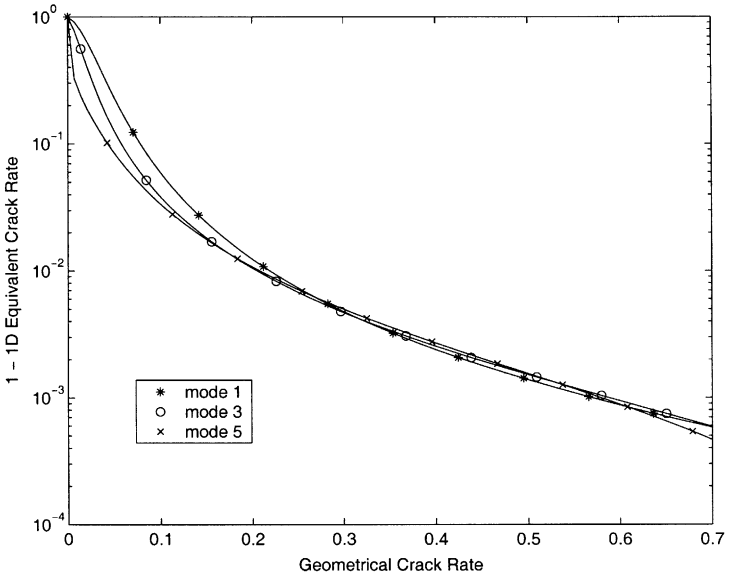

Fig. 6. 1-D-SPR model—equivalent crack rate expressed as a function of the geometrical open-crack rate for the first odd eigenfrequencies.

the Fourier transform of these non-linear responses allows one to determine the eigenfrequency changes between the open crack and the breathing crack. As the non-linear behaviour generated by a breathing crack is relatively weak, the Fourier analysis of the computed impulse responses leads to frequency responses that can be used to correctly estimate the eigenfrequencies for breathing crack conditions.

Fig. 7 presents the comparison of the evolution of the first three odd eigenfrequencies obtained with the 2-D model, respectively, considering an open and a breathing crack.

The breathing crack leads to a reduction of the eigenfrequencies considered which is less than the reduction obtained with the open crack. However, this difference seems to lower with the rank of the eigenfrequency.

Figs. 8 and 9 present the comparison of the evolution of the first three odd eigenfrequencies obtained with the 1-D-EF and the 1-D-SDR models, respectively, considering an open and a breathing crack. These results illustrate the ability of 1-D models to accurately represent the eigenfrequency shifts resulting from the presence of a breathing crack in a beam. When compared, the shifts obtained with the 2-D model and both 1-D models are quite similar, thus confirming the high level of accuracy obtained with 1-D models. However, this accuracy is the result of the updating, by means of the 2-D model results, of the equivalent open-crack rate in both 1-D models.

4. Computation of non-linear effects resulting from a breathing crack

The three proposed models were then used to simulate numerically the non-linear behaviour of a breathing crack at the middle point of the simply supported beam in bending vibrations. The

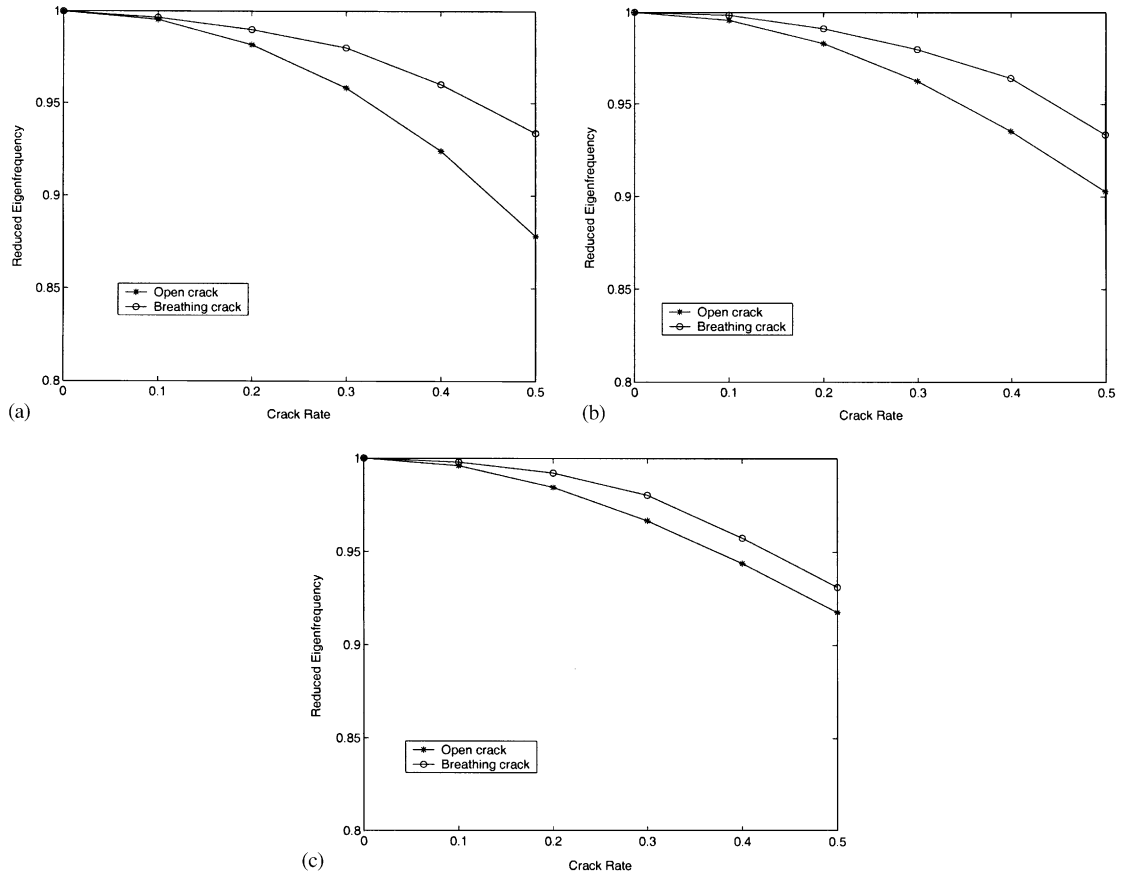

Fig. 7. Evolution of the first three odd eigenfrequencies obtained with the 2-D model, considering an open crack and a breathing crack: (a) eigenfrequency 1, (b) eigenfrequency 3, (c) eigenfrequency 5.

observation point is arbitrarily located at $x_o = 0.70L$ and the excitation point is arbitrarily located at $x_e = 0.32L$. It is represented by a point source of shearing force, the magnitude of which may be expressed as a function of time as follows:

$$F_e(t) = \sin(2\pi f_b t) + \sin(2\pi f_h t), \tag{12}$$

where $f_b = 114$ Hz and $f_h = 1204$ Hz.

Excitation frequency f_b is very close to the first eigenfrequency of the simply supported beam. Excitation frequency f_h is far from any eigenfrequency in that range, as well as any harmonic of the first eigenfrequency. It has been chosen to be between the third, around 1000 Hz, and the fourth, around 1740 Hz, eigenfrequencies of the sound simply supported beam.

This judicious choice also allows one to avoid risks of coincidence between modulation frequencies: $f_{h-b} = f_h - f_b = 1090$ Hz and $f_{h+b} = f_h + f_b = 1318$ Hz, and harmonic frequencies of the first eigenfrequency, respectively: $9f_b = 1026$ Hz, $10f_b = 1140$ Hz, $11f_b = 1254$ Hz and $12f_b = 1368$ Hz.

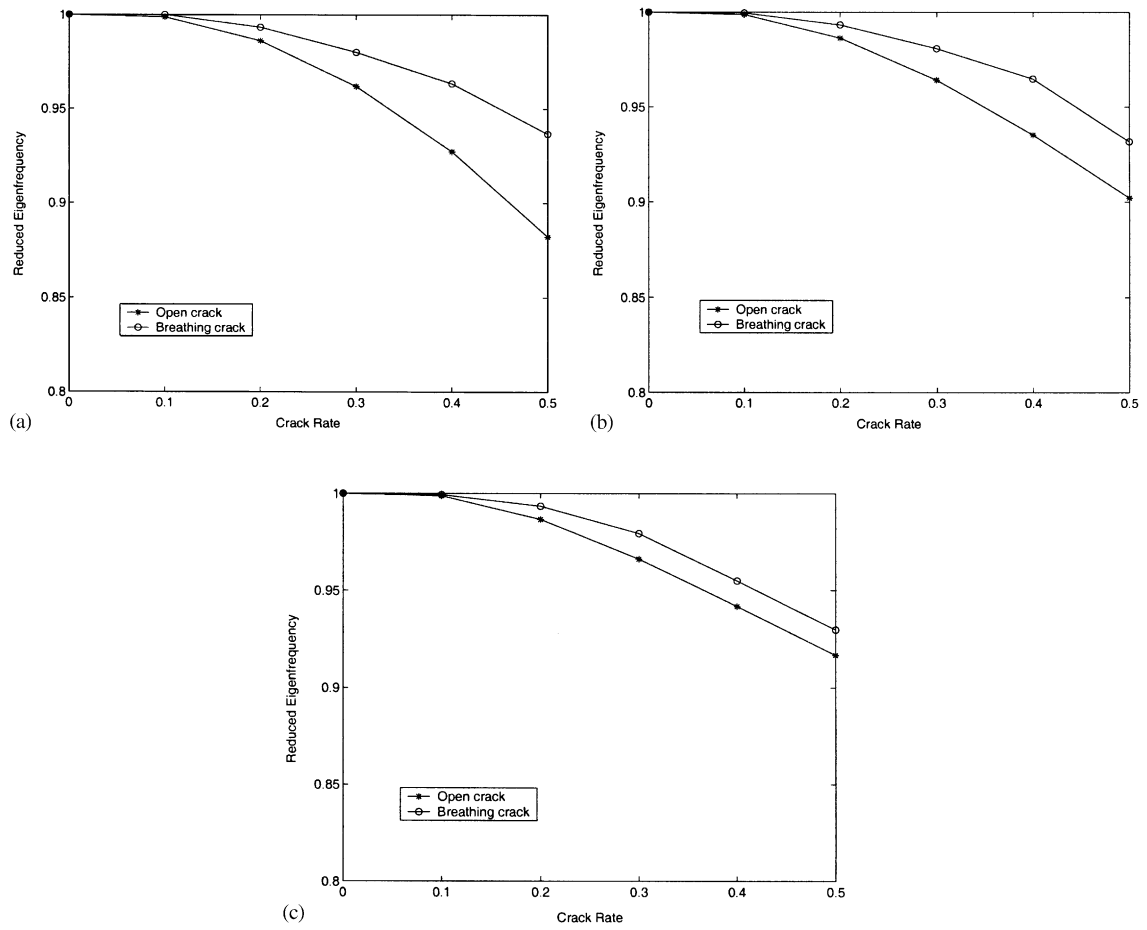

Fig. 8. Evolution of the first three odd eigenfrequencies obtained with the 1-D-EF model, considering an open crack and a breathing crack: (a) eigenfrequency 1, (b) eigenfrequency 3, (c) eigenfrequency 5.

The magnitude of the frequency response of the bending vibration displacement at point x_o is then obtained from the Fourier transform of the time dependent displacement at that point. Fig. 10 presents a frequency response obtained with the 2-D model for a breathing crack with a geometrical crack rate of 0.2.

As shown in Fig. 10, the following magnitudes are used to define two distinct damage rates that may describe the evolution of the size of a possible crack. A_b and A_h, respectively, are the magnitudes obtained at the low and high excitation frequencies f_b and f_h. A_{ib} denotes the magnitude obtained at the harmonic frequency of rank i. A_{h-b} and A_{h+b}, respectively, denote the magnitudes obtained at modulation frequencies f_{h-b} and f_{h+b}. It is interesting to notice in Fig. 10 that the odd rank harmonics of the low excitation frequency do not show. As the breathing crack generates a stiffness loss whose time dependency is numerically represented by a periodic piecewise constant function, its Fourier transform is essentially constituted of lobes located at the

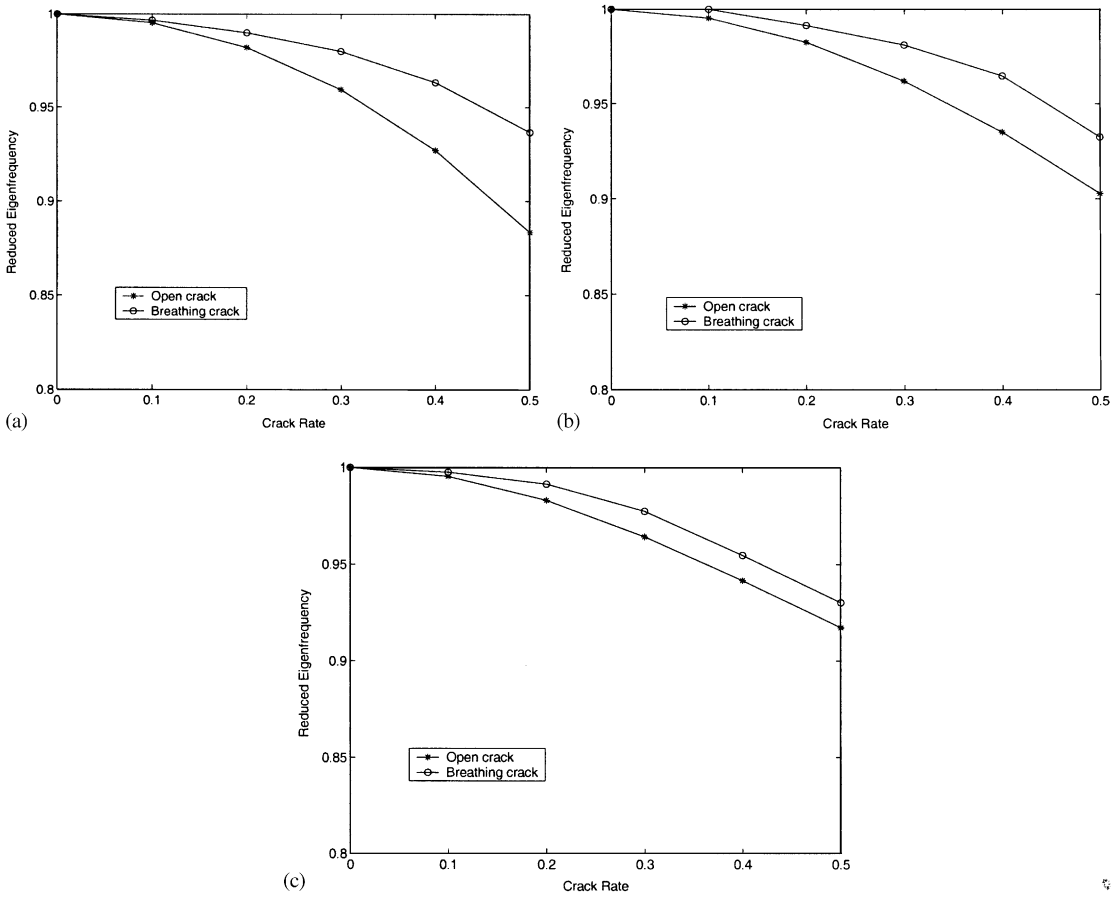

Fig. 9. Evolution of the first three odd eigenfrequencies obtained with the 1-D-SPR model, considering an open crack and a breathing crack: (a) eigenfrequency 1, (b) eigenfrequency 3, (c) eigenfrequency 5.

even rank harmonic frequencies. However, for larger crack rates, the odd rank harmonics of the low excitation frequency also emerge.

Let τ_H be the harmonic damage rate (HDR) associated to the geometrical crack rate of the beam, which is dimensionless. It is determined from the magnitudes obtained at the observation point, as follows:

$$\tau_H = \frac{1}{n-1} \frac{\sum_{i=2}^{n} A_{ib}^2}{A_h A_b}. \tag{13}$$

Let τ_M be the dimensionless modulation damage rate (MDR) associated to the geometrical crack rate. It is determined from the magnitudes obtained at the observation point, as follows:

$$\tau_M = \frac{1}{2} \frac{A_{h+b}^2 + A_{h-b}^2}{A_h A_b}. \tag{14}$$

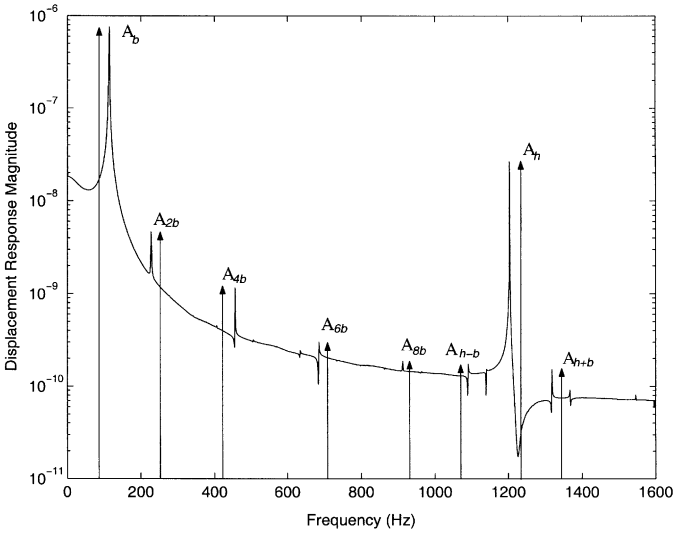

Fig. 10. Frequency response magnitude obtained with the 2-D model for a breathing crack with a geometrical crack rate of 0.2.

Figs. 11 and 12, respectively, illustrate the evolution of the HDR and the MDR, for the three models considered, with the geometrical crack rate.

For crack rate values beyond 10%, the HDR and the MDR grows in a monotonic way with the geometrical crack rate, for all models considered. For a crack rate increase from 10% to 20%, the HDR increases by a factor 6, whereas the MDR increases only by a factor 1.7. For a crack rate increase from 20% to 40%, the HDR increases by a factor 13, whereas the MDR increases only by a factor 4.8. However, this result should be tempered by the fact that a simply supported beam was being considered. Within these limits, the harmonic frequencies of the first eigenfrequency coincide with, or remain close to, the higher rank natural eigenfrequencies of the sound beam, thus increasing the harmonic frequency magnitudes due to the non-linear effects of the breathing crack. Both damage rates, HDR and the MDR, seem to constitute good descriptors of the geometric crack rate, as they grow in a monotonic way, and their growth factors are equal to or larger than the crack rate growth factor. Concerning the 1-D simulation models under consideration, they lead to damage rate results that are very close to the ones obtained with the 2-D model. This result shows that the non-linear behaviour generated by the crack can accurately be represented by a 1-D model. However, for small values of the crack rate, the 1-D-EF model tends to underestimate the damage rates. When compared to the 2-D damage rate, the 1-D-SPR model leads to very similar results.

5. Conclusion

The numerical approaches that have been developed in this paper were devoted to the analysis of the dynamic behaviour of both open and breathing cracks in a flexural vibrating beam and its

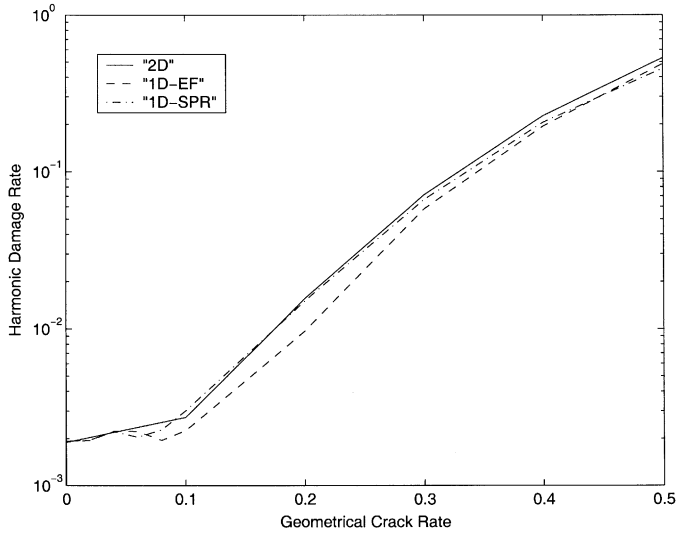

Fig. 11. Evolution of the 'HDR', for the three models considered as a function of the geometrical crack rate.

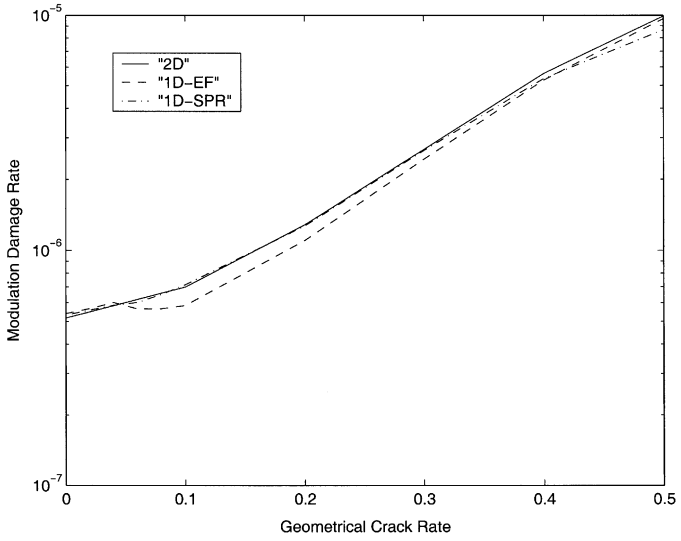

Fig. 12. Evolution of the 'MDR', for the three models considered as a function of the geometrical crack rate.

effects on the subsequent frequency response. For the breathing crack, the non-linear effects have been more precisely examined, and descriptors for the detection of the early presence of a crack have been proposed.

Three finite element models were implemented: two simple one-dimensional models, respectively, 1-D-EF and 1-D-SPR, and one two-dimensional model denoted 2-D. These 1-D models were first tuned by means of modal results obtained with the 2-D finite-element model of a open-crack beam. When tuned, both 1-D models were used to represent the dynamic behaviour of

a breathing crack. Both 1-D models considered, accurately simulate the non-linear effects of the breathing crack, as the subsequent frequency response magnitudes at the observation point correctly approximates the corresponding 2-D magnitudes, for the various geometrical crack rates being considered. For all the models, considered, the magnitudes of the harmonic frequency lobes of the low excitation frequency are quite visible and seem to emerge prior to the modulation lobes. The modulation frequency lobes around the high excitation frequency also grow in a monotonic way with the geometrical crack rate. However, the modulation lobes are quite visible, even for very low crack rates such as a few per cent.

Based upon the frequency response magnitudes computed for various geometrical crack rates, two distinct damage rates have been proposed as descriptors to characterize the presence of the crack in the beam: the HDR and the MDR. The HDR and the MDR grow in a monotonic way with the geometrical crack rate over 10%. The HDR presents a larger slope than the MDR, making it more sensitive to the presence of a crack in the beam. Therefore, it appears that both damage rates, HDR and the MDR, seem to constitute good descriptors of the geometrical crack rate, as they grow in a monotonic way, and their growth factors are equal or larger than the crack rate growth factor. Damage rate results computed with 1-D simulation models are very close to that with 2-D model, which shows that the non-linear behaviour generated by the crack can accurately be represented by a simple 1-D model that is properly tuned.

Nevertheless, experiments showed that the ideal behaviour of a breathing crack, such as simulated in this analysis, may have a weak probability of occurrence in the industrial world. Most of the time, some static traction or compression stresses apply to the crack region in such a way that the time dependency of the stiffness loss at the crack point is slightly different from a periodic piecewise constant function, and its magnitude will also usually depend upon the crack geometry in a non-linear way. However, the measured effects of the non-linear dynamic behaviour of a breathing crack, such as the HDR and the MDR, are not very sensitive to pre-stressing conditions. As long as the crack opens and closes with the dynamic motion, they will grow in a monotonic way with the crack rate, whatever pre-stressing conditions they may be.

Acknowledgements

This work was supported by the Non-Destructive Evaluation Center of the Electric Power Research Institute in Charlotte, NC, USA.

References

[1] S. Christides, A.S. Barr, One dimensional theory of cracked Bernoulli–Euler beams, International Journal of the Mechanical Sciences 26 (1984) 639–648.

[2] J. Fernadez-Saez, L. Rubio, C. Navarro, Approximate calculation of the fundamental frequency for bending vibrations of cracked beams, Journal of Sound and Vibration 225 (2) (1999) 345–352.

[3] W. Ostachowicz, M. Krawczuk, On modelling of structural stiffness loss due to damage, Key Engineering Materials 204–205 (2001) 185–200.

[4] P. Rizos, N. Aspragathos, A. Dimarogonas, Identification of crack location and magnitude in a cantilever beam from the vibration modes, Journal of Sound and Vibration 138 (1990) 381–388.

[5] P.Y. Narkis, Identification of crack location in vibrating simply supported beams, Journal of Sound and Vibration 172 (1994) 549–558.
[6] A.K. Pandey, M. Biswas, Experimental verification of flexibility difference method for locating damage in structures, Journal of Sound and Vibration 184 (2) (1995) 311–328.
[7] S. Masoud, M. Jarrah, M. Al-Maamory, Effect of crack depth on the natural frequency of a prestressed fixed–fixed beam, Journal of Sound and Vibration 214 (2) (1998) 201–212.
[8] S. Cheng, X. Wu, W. Wallace, A. Swamidas, Vibrational response of a beam with a breathing crack, Journal of Sound and Vibration 225 (1) (1999) 201–208.
[9] A. Dimarogonas, S. Paipetis, Analytical Methods in Rotor Dynamics, Applied Science Publishers, London, 1983.
[10] O. Buck, W. Morris, J. Richardson, Acoustic harmonic generation at unbounded interfaces and fatigue cracks, Applied Physics Letters 33 (5) (1978) 371–373.
[11] W. Morris, O. Buck, R. Inman, Acoustic harmonic generation due to fatigue damage in high strength aluminium, Applied Physics Letters 50 (11) (1979) 6737–6741.
[12] O.S. Jun, H.J. Eun, Y.Y. Earmme, C.W. Lee, Modelling and vibration analysis of a simple rotor with a breathing crack, Journal of Sound and Vibration 155 (2) (1992) 273–290.
[13] J. Wauer, On the dynamics of cracked rotors: a literature survey, Applied Mechanics Review 43 (1) (1990) 13–17.
[14] R. Gasch, A survey of the dynamic behaviour of a simple rotating shaft with a transverse crack, Journal of Sound and Vibration 160 (2) (1992) 313–332.
[15] G.E. Dace, O. Buck, R.B. Thompson, Using non-linear acoustics for non destructive materials characterization and evaluation, in: P.J. Raju (Ed.), Vibro-Acoustic Characterization of Materials and Structures, NCA, Vol. l4, ASME, New York, 1992, pp. 221–225.
[16] D.M. Donskoy, K. Ferroni, A.M. Sutin, K. Sheppard, A non-linear acoustic technique for crack and corrosion detection in reinforced concrete, in: R.E. Green Jr. (Ed.), Non-destructive Characterization of Material VIII, Plenum Press, New York, 1998, pp. 555–560.
[17] A.M. Sutin, D.M. Donskoy, Vibro-acoustic modulation non-destructive evaluation technique, in: G.A. Geithman, G.E. Georgeson (Eds.), Nondestructive Evaluation of Aging Aircraft, Airports and Aerospace Hardware II, Proceedings of SPIE—The International Society of Optical Engineering, Vol. 3397, SPIE, Bellingham, WA, 1998, pp. 226–237.
[18] A.E. Ekimov, I.N. Didenkulov, V.V. Kazakov, Modulation of torsional waves in a rod with a crack, Journal of the Acoustical Society of America 106 (3) (1999) 1289–1292.
[19] V. Zaitsev, P. Sas, Non-linear response of a weakly damaged metal sample: a dissipative modulation mechanism of vibro-acoustic interaction, Journal of Vibration and Control 6 (2000) 803–822.
[20] K. Krzywosz, S. Walker, Non-linear vibro-acoustic screening system for detecting cracks in pipe socket welds, E.P.R.I. – N.D.E. Center, Charlotte, NC, Final Report TR-110427, 1999.
[21] S. Cambier, E. Luzzato, Prise en compte des incertitudes dans les calculs vibratoires de tuyauteries—approches fonctionnelles et probabilistes, Table Ronde MV2: Approche Robuste en Dynamique des Structures, 2000.